

CLaDMoP: Learning Transferrable Models from Successful Clinical Trials via LLMs

Yiqing Zhang
yzhang37@wpi.edu
Worcester Polytechnic Institute
Worcester, MA, USA

Xiaozhong Liu
xliu14@wpi.edu
Worcester Polytechnic Institute
Worcester, MA, USA

Fabricio Murai
fmurai@wpi.edu
Worcester Polytechnic Institute
Worcester, MA, USA

ABSTRACT

Many existing models for clinical trial outcome prediction are optimized using task-specific loss functions on trial phase-specific data. While this scheme may boost prediction for common diseases and drugs, it can hinder learning of generalizable representations, leading to more false positives/negatives. To address this limitation, we introduce CLaDMoP, a new pre-training approach for clinical trial outcome prediction, alongside the Successful Clinical Trials dataset (SCT), specifically designed for this task. CLaDMoP leverages a Large Language Model—to encode trials’ eligibility criteria—linked to a lightweight Drug-Molecule branch through a novel multi-level fusion technique. To efficiently fuse long embeddings across levels, we incorporate a grouping block, drastically reducing computational overhead. CLaDMoP avoids reliance on task-specific objectives by pre-training on a “pair matching” proxy task. Compared to established zero-shot and few-shot baselines, our method significantly improves both PR-AUC and ROC-AUC, especially for phase I and phase II trials. We further evaluate and perform ablation on CLaDMoP after Parameter-Efficient Fine-Tuning, comparing it to state-of-the-art supervised baselines, including MEXA-CTP, on the Trial Outcome Prediction (TOP) benchmark. CLaDMoP achieves up to 10.5% improvement in PR-AUC and 3.6% in ROC-AUC, while attaining comparable F1 score to MEXA-CTP, highlighting its potential for clinical trial outcome prediction. **Code and SCT dataset can be downloaded from** <https://github.com/murai-lab/CLaDMoP>.

CCS CONCEPTS

• **Computing methodologies** → **Knowledge representation and reasoning**; **Supervised learning by classification**; **Neural networks**; **Unsupervised learning**.

KEYWORDS

Clinical Trial Outcome Prediction; Multi-modal Data Fusion; Self-Supervised Pre-training; LLMs; Representation Learning.

ACM Reference Format:

Yiqing Zhang, Xiaozhong Liu, and Fabricio Murai. 2025. CLaDMoP: Learning Transferrable Models from Successful Clinical Trials via LLMs. In *Proceedings of 31th ACM SIGKDD Conference on Knowledge Discovery and Data Mining (KDD’25)*. ACM, New York, NY, USA, 12 pages. <https://doi.org/XXXXXXX.XXXXXXX>

1 INTRODUCTION

Clinical trial outcome prediction is a challenging task due to the complexity of biological systems. Specifically, factors such as heterogeneity [8, 23] among patients, unclear disease mechanisms, and differing responses to treatments make accurate predictions particularly difficult. Additionally, regulatory and ethical constraints [9, 24], lengthy approval processes [5], and the high costs of recruitment further increase time and expenses [2, 6, 22]. Despite ongoing challenges faced by the traditional clinical trial prediction methods, the growing availability of historical data on both successful and failed drugs offers a unique opportunity to leverage sophisticated artificial intelligence models for more accurate predictions. These advanced methods could improve prediction success rates, enabling more effective resource allocation, prioritizing trials with a higher likelihood of positive outcomes, and ultimately streamlining the drug development process.

Recent deep learning approaches for clinical trial outcome prediction mainly focus on improving mechanisms for harnessing multi-modality data. For example, Hierarchical Interaction Network (HINT) [12] integrates multimodal data — such as drug molecules, disease information, trial protocols, and wet lab data (including pharmacokinetics properties like absorption, distribution, metabolism, excretion, and toxicity) — by extracting and fusing their representations through a human-designed graph model to enhance outcome predictions. MEXA-CTP [45] employs soft and hard masks to selectively extract relevant information. The domain-conditioned masks are optimized by Cauchy loss [27] and leverage masked cross-attention layers to model interactions between pairs of domains, each represented by a module referred to as “mode expert”. This framework enables the model to learn relationships between drug molecules, diseases, and trial protocols directly from data, rather than relying on hard-coded human priors.

Limitations of State-of-the-Art Approaches. Many models are optimized using task-specific loss functions, which can hinder the learning of robust representations. This is especially problematic for rare or new diseases, for which limited labeled data is available. Furthermore, while a task-specific loss function may improve performance for common diseases and drugs, it leads to a decrease in the model’s ability to generalize to special cases (increase in false positives or false negatives), limiting its robustness and adaptability to new, unseen scenarios. Meanwhile, all prior works, like HINT

Permission to make digital or hard copies of all or part of this work for personal or classroom use is granted without fee provided that copies are not made or distributed for profit or commercial advantage and that copies bear this notice and the full citation on the first page. Copyrights for components of this work owned by others than the author(s) must be honored. Abstracting with credit is permitted. To copy otherwise, or republish, to post on servers or to redistribute to lists, requires prior specific permission and/or a fee. Request permissions from permissions@acm.org.

KDD’25, August 03–07, 2025, Toronto, Canada

© 2025 Copyright held by the owner/author(s). Publication rights licensed to ACM.

ACM ISBN 978-1-4503-XXXX-X/2018/06...\$15.00

<https://doi.org/XXXXXXX.XXXXXXX>

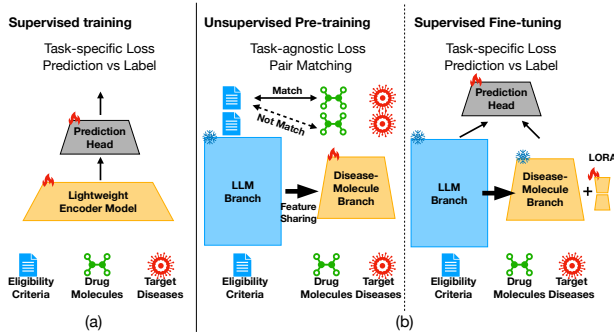


Figure 1: (a) Recent work has focused on using a lightweight encoder model and a prediction head trained with a task-specific loss due to limitations in the availability of labeled data. (b) In contrast, CLaDMoP follows a two-stage training paradigm. It incorporates a large language model (LLM branch) and a lightweight attention model (Disease-Molecule branch), sharing knowledge from the former to the latter. (b-left) Pre-training stage: uses pair matching as a proxy task and a task-agnostic loss for optimization. (b-right) Fine-tuning stage: evaluation performance is further improved by training a prediction head and LoRA layers for DM branch.

and MEXA-CTP, heavily rely on task-specific losses, which require substantial human effort to manually annotate historical data.

Our Approach. We present a first-in-class method, Contrastive Language Drug Molecule Pretraining (CLaDMoP), aimed at improving clinical trial outcome prediction performance by incorporating self-supervised learning as a pre-training stage. To create the pre-training dataset, we link trials from ClinicalTrials.gov¹ with drug synonyms from DrugBank², ensuring all Successful Clinical Trials (SCT) are accurately represented. Details can be found in Section 3.2.

Similar to the structure of the CLIP model [31], CLaDMoP consists of two branches (see Figure 1(b)): the Large Language Model (LLM) branch utilizes an LLM to extract information from eligibility criteria, while the Drug-Molecule (DM) branch features a custom transformer-based model designed to learn a joint representation from drug molecules and target diseases.

We freeze the LLM branch and optimize the parameters in the DM branch to maximize the similarity between successful pairs of eligibility criteria embeddings and drug-disease embeddings, while minimizing similarity to all other combinations. We treat the pair matching of all successful clinical trials as a proxy task, and adopt the InfoNCE loss [28] to optimize this objective. The LLM branch consists of transformers blocks divided into multiple levels. Every level, except the last, shares distilled knowledge with the DM branch through multi-level fusion. This would typically incur high computational costs due to the increase in token sequence length at every level, causing the computational cost of attention layers to grow disproportionately. To address this issue, we introduce a grouping layer that reduces the sequence length by projecting them to trainable centroid tokens via cross-attention. By stacking

multiple grouping layers to form a grouping block, CLaDMoP progressively reduces the number of tokens while maintaining superior performance compared to HINT and MEXA-CTP.

We further enhance the performance of our model via Parameter-Efficient Fine-Tuning (PEFT) [15]. We fix the parameters from the pre-training stage and train the Low-Rank Adaptation (LoRA) [17] layers for the attention layers in DM branch, along with a prediction head. The proposed method outperforms the current state-of-the-art results on the Trial Outcome Prediction (TOP) benchmark.

In sum, **our main contributions are:**

- We propose CLaDMoP, a new pre-training approach for clinical trial outcome prediction, and construct the Successful Clinical Trials (SCT) dataset, specifically designed for the pre-training task. Compared to established zero-shot and few-shot baselines, our method demonstrates significant improvements in PR-AUC and ROC-AUC, particularly in phase I and phase II.
- We incorporate a pre-trained LLM model in CLaDMoP, paired with a lightweight model in the DM branch. We extract intermediate LLM embeddings and fuse them to the embeddings from the DM branch through a novel multi-level fusion technique. By implementing a grouping block to aggregate the information and control the sequence length of intermediate tokens, we drastically reduce the overall training complexity.
- We evaluate and perform ablation on CLaDMoP after PEFT on the downstream task against several state-of-the-art baselines, including MEXA-CTP, using the TOP dataset from phase I, II, and III clinical trials. CLaDMoP achieves up to 10.5% and 3.6% improvement in terms of PR-AUC, and ROC-AUC, respectively, while matching MEXA-CTP’s F1 score.
- We analyze the accuracy and absolute gain in correct predictions for new diseases, comparing CLaDMoP with the previous state-of-the-art MEXA-CTP. We demonstrate that CLaDMoP learns generalizable embeddings through task-agnostic loss and can seamlessly adapt to new clinical trials. Our comparison with MEXA-CTP on the subset of new diseases reveals that CLaDMoP outperforms MEXA-CTP by 13.63% in phase I, 8.02% in phase II, while matching its performance in phase III in terms of accuracy.

2 PRELIMINARIES

This section formally defines key elements of the clinical trial outcome prediction task and the notation used throughout the paper.

The standard clinical trial outcome prediction task involves **Drug Molecules** \mathcal{M} , **Target Diseases** \mathcal{D} and **Eligibility Criteria** \mathcal{C} . Given a combination of $(\mathcal{M}, \mathcal{D}, \mathcal{C})$, our goal is to predict the final outcome of the clinical trial, i.e. whether it succeeded or not.

Definition 2.1. **Drug Molecules** refer to chemical compounds that are designed or discovered to have therapeutic effects on biological systems. They can interact with specific biological targets, such as proteins or enzymes, to modify physiological processes and treat diseases. We denote the set of drug molecules in clinical trial

¹<https://clinicaltrials.gov/>

²<https://go.drugbank.com/>

j without considering quantities or percentuals³ by

$$\mathcal{M}^{(j)} := \{M_1^{(j)}, M_2^{(j)}, \dots, M_{M_j}^{(j)}\}, \quad j \in [1..N], \quad (1)$$

where each $M_i^{(j)}; i \in [1..M_j]$ is a drug molecule which might have an effect on one or more target diseases.

Definition 2.2. Target Diseases are coded using the ICD-10 (International Classification of Diseases, 10th revision⁴) system, which provides a hierarchical structure for categorizing diseases based on their characteristics (e.g., infectious diseases, cardiovascular diseases, cancers). We denote the combination of target diseases in clinical trial j by

$$\mathcal{D}^{(j)} := \{D_1^{(j)}, D_2^{(j)}, \dots, D_{d_j}^{(j)}\} \quad (2)$$

where $D_i^{(j)}; i \in [1..d_j]$ is an individual ICD-10 diagnosis code.

Definition 2.3. Eligibility Criteria are specific requirements that participants must meet to be included in the study. They are typically structured text data, including inclusion criteria and exclusion criteria, collectively denoted by $\mathcal{C}^{(j)}$ for clinical trial j .

To avoid clutter, we will omit (j) unless there is risk of ambiguity.

Definition 2.4. Clinical Trial Outcome. Clinical trials typically evaluate the effectiveness of a drug based on a variety of metrics related to the symptoms they aim to alleviate, as well as broader health and safety considerations. These metrics can include specific symptom scores, biomarker levels, or other health indicators. The outcome is often a binary label y , where a positive outcome $y = 1$ indicates success (i.e., drug was effective or safe), and a negative outcome $y = 0$ indicates otherwise.

Definition 2.5. (Clinical Trial) Pre-training. We propose a new task where the goal is to minimize a joint loss $\mathcal{L}_{\text{pre-training}}$ across different modalities, encouraging the model to learn a robust representation. The objective function is defined as:

$$\theta^*, \phi^* = \arg \min_{\theta, \phi} \mathcal{L}_{\text{pre-training}}(f(\mathcal{M}, \mathcal{D}; \theta), g(\mathcal{C}; \phi)), \quad (3)$$

where $f(\mathcal{M}, \mathcal{D}; \theta)$ learns a joint representation from drug molecules (\mathcal{M}) and target diseases (\mathcal{D}), and is parameterized by θ ; $g(\mathcal{C}; \phi)$ learns to represent eligibility criteria \mathcal{C} , and is parameterized by ϕ . In our approach, we fix parameters ϕ (LLM branch) during training.

Definition 2.6. (Clinical Trial) Fine-tuning. The fine-tuning objective is to minimize a supervised loss function $\mathcal{L}_{\text{fine-tuning}}$ by optimizing the model’s parameters. The task is formalized as:

$$\psi^* = \arg \min_{\psi} \mathcal{L}_{\text{fine-tuning}}(H(f(\mathcal{M}, \mathcal{D}), g(\mathcal{C})); \psi), \quad (4)$$

where H is a prediction head parameterized by ψ , and the loss function $\mathcal{L}_{\text{fine-tuning}}$ is designed to optimize the model’s performance on the task at hand.

3 PROPOSED METHOD

Inspired by models like CLIP [31] and its variants [10, 36], which effectively align vision and language representations, we introduce CLaDMoP to harness the strengths of self-supervised pre-training and large language models. This framework consists of two branches: the Large Language Model (LLM) branch and the Disease-Molecular (DM) branch. The LLM branch aims to capture the structural and semantic information from eligibility criteria, while the DM branch focuses on modeling the relationship between drug molecules and target diseases. To fully utilize feature extraction capabilities from LLM model, we design a multi-level feature fusion scheme to integrate embeddings from the LLM to the DM branch. After each level of feature fusion, we apply grouping layers to progressively reduce the number of tokens, preventing linear growth in token length and quadratic growth in attention block complexity during multi-level fusion.

We employ a two-stage training paradigm to enhance clinical trial outcome prediction performance. The first stage involves self-supervised pre-training, where the model learns robust representations for successful pairs of $(\mathcal{M}, \mathcal{D}, \mathcal{C})$ via a pair-matching proxy task. In the second stage, we further improve performance with supervised fine-tuning. Our optimization strategy is designed to effectively train the model in under scarce labeled data scenarios.

3.1 Model Architecture

3.1.1 LLM branch. The LLM branch is responsible for processing eligibility criteria input. We choose BioGPT [26] as the LLM model due to its specialization in biomedical text, which enables efficient extraction for the embedding of the eligibility criteria. BioGPT leverages advanced natural language processing (NLP) to understand and interpret domain-specific language, such as inclusion and exclusion criteria, medical history, and other qualification requirements. BioGPT’s last layer embedding of the eligibility criteria will be denoted as $U^C = \text{BioGPT}(\mathcal{C})$.

To further distill knowledge from the BioGPT model, we consider intermediate embeddings obtained at three different levels, going from coarser (shallower) to finer (deeper) representations. Specifically, we consider sequences of 6 consecutive attention blocks, where the first 6 blocks generate coarse level embeddings U_{coarse}^C , then forwarded through the next 6 blocks to generate medium level embeddings U_{medium}^C and, finally, through the following 6 blocks (for a total of 18 blocks) to generate fine level embeddings U_{fine}^C . These multi-level embeddings enable us to capture varying detail and context within the text, enhancing the richness of the representation.

3.1.2 DM branch. Learns a joint representation for drug molecules and target disease (details can be found in Appendix A), aggregating information from the LLM branch.

Drug Molecules Embedding. We utilize DeepChem [33] to encode each molecule expressed as a SMILES string. For different molecules, we add learnable positional embeddings to distinguish whether the segments come from the same molecule. We utilize

³In clinical trial data, ingredients’ quantities or percentuals are not always informed [38], as the main focus is on the presence of molecules relevant to the study.

⁴<https://www.icd10data.com/ICD10CM/Codes>

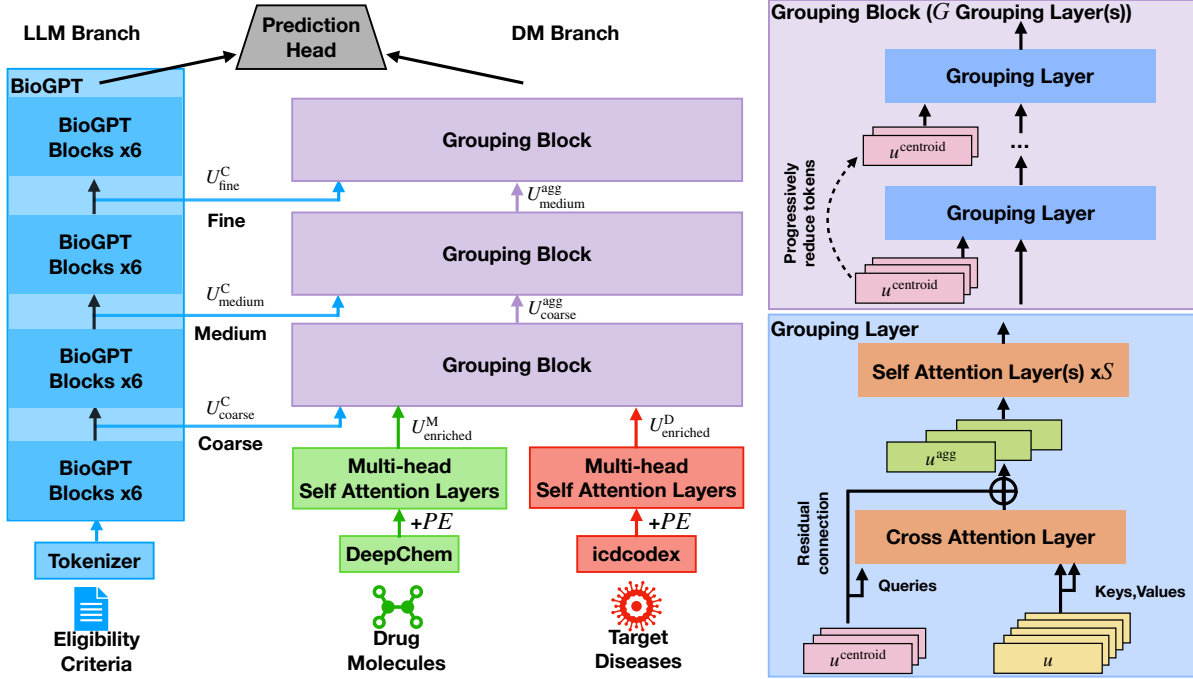


Figure 2: (Left) CLaDMoP consists of two branches: the LLM branch and the DM branch. The prediction head is a three-layer residual network, which is trained during the PEFT stage. Further details are provided in Section 3.1. (Right-top) The grouping block enables the model to fuse information from the LLM branch. Each grouping block consists of G grouping layer(s), where the number of centroids is progressively reduced at each layer. The structure of the grouping layer is shown in (Right-bottom), while S indicates the number of the self-attention layer in a grouping layer, with further details provided in Section 3.1.2. Note that u is a single token belonging to token sequence U .

self-attention layers to further enrich the embedding. The drug molecule embedding is denoted by $U_{enriched}^M$.

Target Disease Embedding. We encode disease hierarchical information using the ICD-CODEX package⁵. We add learnable positional embeddings shared by diseases that belong to the same ICD-10 category. The combined embedding is in turn forwarded through self-attention layers, yielding the final target disease embedding, denoted by $U_{enriched}^D$.

Multi-level feature fusion. To fully incorporate the intermediate embeddings across all levels without significantly increasing the computational cost, we introduce a grouping block to merge and aggregate information from the LLM branch into the DM branch.

Grouping Layer. We employ a cross-attention mechanism to integrate information from input tokens into centroids. To facilitate this process, we introduce trainable centroid tokens, initialized from the Gaussian distribution $N(0, 1)$. These centroids generate queries via cross-attention layer, enabling them to efficiently fuse relevant information from the input tokens (i.e., drug molecule, target disease, and eligibility criteria tokens) as follows:

$$U^{agg} = \text{softmax} \left(\frac{U^{centroid} W^Q (U W^K)^T}{\sqrt{d_k}} \right) U W^V, \quad (5)$$

where U represents the input tokens which generate keys and values via W^K and W^V , where $U \in \{U_{enriched}^M, U_{enriched}^D, U_x^C, U_{x-1}^{agg}\}$, $x \in \{\text{coarse, medium, fine}\}$, $U^{centroid}$ indicates the centroid tokens which generate queries, and d_k is the embedding dimension. Information is aggregated based on the attention map produced by the softmax function. By using this cross-attention mechanism, we ensure that the fused output U^{agg} always has the same sequence length as $U^{centroid}$, which dramatically reduces the computational overhead (a detailed study of the complexity analysis is presented in Section 4.4). Additionally, to mitigate potential losses in embedding quality, we stack S self-attention layers on the top of the cross attention layer. This design not only helps manage sequence length but also prevents the loss of critical information. Additionally, to ensure that the model captures input tokens from diverse sources, we add learnable positional embeddings to distinguish them.

Grouping Block. We stack G grouping layers to form a grouping block. The purpose of stacking these grouping layers is to progressively reduce the number of centroids. Specifically, in each layer, we reduce the number of centroids by half compared to the previous layer, ensuring that all key information is retained.

The DM branch first fuses U_{coarse}^C , followed by U_{medium}^C and U_{fine}^C . We add layer normalization to the final output to ensure it matches the scale of the LLM branch. The final output tokens of the DM branch are denoted by $U^{\mathcal{D}, \mathcal{M}}$.

⁵<https://github.com/icd-codex/icd-codex>

3.2 Pre-training Stage

In the pre-training stage, our goal is to train the model to correctly identify a match when $(\mathcal{M}, \mathcal{D}, C)$ comes from a successful trial. This is equivalent to ensuring that the match has a higher similarity score than both mismatched pairs and failed trials. To reduce the effort required for manual labeling, we adopt a more efficient approach for collecting a new dataset that focuses solely on Successful Clinical Trials, SCT dataset.

Table 1: Successful Clinical Trials, SCT dataset statistics.

Statistic	Value
Number of drugs	4,289
Number of diseases	3,326
Avg. words in eligibility criteria	364
Unique drug combinations	2,902
Unique disease combinations	951

Dataset. We construct this dataset by linking data from ClinicalTrials.gov⁶ and DrugBank⁷. While each clinical trial explicitly states the drug name, drug synonyms may appear in related or subsequent trials. To ensure that drug synonyms across multiple trials—especially those related to the same disease—are correctly mapped to the same drug entity, we reference DrugBank to identify synonyms and the target disease. This allows us to establish a sequence of trials for each drug. For drugs already on the market, we assume that all clinical trials from phase I to phase III were successful [3, 7]. Additionally, we assume that a drug progressing to phase $p \in \{II, III, IV\}$ has successfully completed all previous phases⁸. To maintain data integrity, we automatically filter out trials where drugs lack relevant experiments in subsequent phases. For example, if a drug has results from phase I to phase III but no phase IV data, we exclude it from the phase III dataset, as the outcome remains uncertain without validation of the clinical trial’s public records. In contrast, our process is fully automated, reducing the need for manual labeling. Table 1 shows key statistics of the SCT dataset. To prevent data leakage, we ensure that none of the trials in TOP’s test set are included in SCT’s pre-training data. Specifically, we perform a temporal split based on NCTid for train-test separation, analogous to the split done by previous works for TOP.

We freeze the parameters in the LLM branch and train the DM branch using a pair-matching task, where the goal is to predict the correct pairings $(U^C$ and $U^{\mathcal{D}, \mathcal{M}})$. To achieve this, we optimize a symmetric cross-entropy loss over the similarity scores, which is widely used in contrastive representation learning as the InfoNCE loss. We adapt this approach specifically for the clinical trial outcome prediction task shown in Algorithm 1.

3.3 Fine-tuning Stage (using PEFT)

The goal of the PEFT stage is to enable the model to discriminate between successful and failed trials under supervision. To achieve

⁶<https://clinicaltrials.gov/>

⁷<https://go.drugbank.com/>

⁸<https://www.fda.gov/patients/learn-about-drug-and-device-approvals/drug-development-process>

Algorithm 1 Pseudocode for Pre-training Loss

- 1: **Input:** Batch size n , temperature parameter τ
- 2: **Output:** Pre-training loss $\mathcal{L}_{\text{pre-training}}$
- 3: {Identity matrix indicating which pairs are CORRECT matches}
labels = $\text{diag}([1, 1, \dots, 1])_{n \times n}$
- 4: $f_C = \text{Avgpool}(U^C)$ {final eligibility criteria embeddings}
- 5: $f_{\mathcal{D}\mathcal{M}} = \text{Avgpool}(U^{\mathcal{D}, \mathcal{M}})$ {final disease-drug embeddings}
- 6: {Compute logits w/ temperature scaling for all embedding pairs}
logits = $\exp(\tau) \cdot f_C \times f_{\mathcal{D}\mathcal{M}}^\top$
- 7: {Compute cross-entropy over rows}
 $\mathcal{L}_{\text{row}} = \text{cross_entropy}(\text{logits}, \text{labels}, \text{axis} = 0)$
- 8: {Compute cross-entropy over columns}
 $\mathcal{L}_{\text{col}} = \text{cross_entropy}(\text{logits}, \text{labels}, \text{axis} = 1)$
- 9: $\mathcal{L}_{\text{pre-training}} = (\mathcal{L}_{\text{row}} + \mathcal{L}_{\text{col}})/2$ {final pre-training loss}

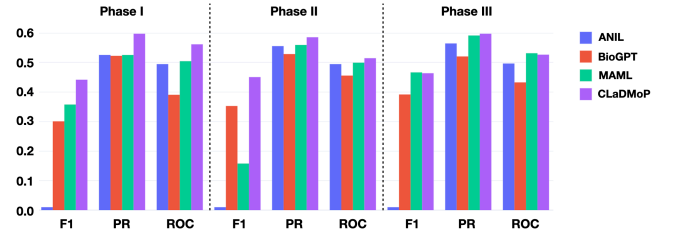


Figure 3: Few-shot learning results for clinical trial outcome prediction for phase I, II and III trials.

this, we apply average pooling to both LLM and DM branches in order to aggregate the information in each. The resulting embeddings from each branch are then concatenated and passed through a prediction head with a sigmoid activation function. This produces a probability score indicating whether the trial is successful or not:

$$\hat{y} = \sigma \left(H_{\text{pred}} \left(\text{concat} \left(\text{Avgpool}(U^C), \text{Avgpool}(U^{\mathcal{D}, \mathcal{M}}) \right) \right) \right), \quad (6)$$

where H_{pred} represents the prediction head. To further improve fine-tuning performance without affecting the parameters from the pre-training stage, we freeze the pre-trained parameters and introduce LoRA layers to the DM branch.

A class-weighted binary cross-entropy loss is used for guiding the model training due to the imbalance of negative/positive pairs:

$$\mathcal{L}_{\text{PEFT}} = -\omega_0 y \log \hat{y} - \omega_1 (1 - y) \log (1 - \hat{y}), \quad (7)$$

where ω_0 (ω_1) is the fraction of negative (positive) labels in the training set.

4 EXPERIMENTS

We meticulously follow the experimental settings described in the Trial Outcome Prediction (TOP) benchmark [12] to evaluate our model for both pre-training stage and fine-tuning stage. In addition, to assess the capabilities of the learning components, we conduct ablation studies to evaluate the importance of different components of our model.

Table 2: Experimental results for outcome prediction for phase I, II, and III trials. Results correspond to averages and standard deviations over 10 bootstrap samples.

	Metric	LR	RF	KNN+RF	XGBoost	AdaBoost	FFNN	HINT	MEXA-CTP	CLaDMoP
Phase I	F1	.503±.017	.519±.017	.522±.014	.624±.016	.633±.015	.614±.009	.604±.009	.713±.027	.713±.019
	PR-AUC	.515±.015	.514±.015	.514±.004	.594±.015	.544±.011	.569±.012	.581±.021	.605±.014	.680±.016
	ROC-AUC	.514±.018	.542±.014	.528±.009	.538±.016	.540±.012	.550±.010	.575±.021	.593±.012	.642±.015
Phase II	F1	.533±.017	.534±.013	.594±.011	.572±.013	.579±.008	.579±.008	.635±.010	.695±.008	.685±.015
	PR-AUC	.560±.012	.573±.015	.583±.014	.585±.015	.586±.013	.586±.013	.608±.011	.635±.015	.683±.012
	ROC-AUC	.567±.016	.576±.010	.583±.016	.601±.003	.589±.013	.601±.012	.623±.012	.638±.005	.647±.018
Phase III	F1	.624±.013	.675±.018	.670±.018	.694±.017	.722±.014	.625±.017	.814±.013	.857±.007	.861±.014
	PR-AUC	.553±.011	.583±.024	.587±.016	.627±.009	.589±.015	.572±.020	.603±.014	.771±.016	.860±.011
	ROC-AUC	.600±.028	.643±.023	.643±.024	.668±.014	.624±.013	.620±.023	.685±.023	.693±.025	.702±.018

4.1 Experimental Settings

To the best of our knowledge, the TOP benchmark is the only publicly available dataset for clinical trial outcome prediction and has been incorporated into TrialBench for the clinical trial approval task. To evaluate the proposed model, we use the TOP benchmark and follow the same strategy for splitting the train, and test sets. Specifically, for each phase, we split the dataset based on the start day of the clinical trials, allocating earlier trials to the train set and using later trials for model evaluation. This approach allows us to evaluate the model’s performance on unseen data from different time periods, helping to assess its generalization ability. During training, we randomly select 15% of the training samples as the validation set to monitor the model’s performance and tune hyperparameters. This protocol is part of the TOP’s experimental design, ensuring consistency and fair comparisons with other studies. For statistics of the data splits, please refer to Appendix B.1.

Evaluation Metrics. We utilize standard evaluation metrics for clinical trial outcome prediction, including F1 score (i.e., the harmonic mean of precision and recall), PR-AUC (i.e., area under the precision-recall curve), and ROC-AUC (i.e., area under the receiver operating characteristic curve). For all three metrics, higher values indicate better performance.

Pre-training Stage. Our Model. We use BioGPT as the eligibility criteria encoder within the LLM branch. In DM branch, we stack four self-attention layers in each attention block to extract features, separately for drug molecules and target diseases. Each attention layer contains 8 attention heads, with an embedding size of 16. We then use 3 grouping blocks to integrate and aggregate information from the LLM branch into the DM branch. Each grouping block consists of a cross-attention layer followed by two self-attention layers. The number of centroids starts at 100 and is gradually halved, ultimately reducing to 25 at the final block.

Training. All the parameters in the LLM branch are fixed during pre-training. We optimized the DM branch with Adam using default values for β_1 and β_2 . Based on our results from hyperparameter tuning (see Appendix C.3), we set the batch size to 128 and use a fixed learning rate 10^{-4} for training. The temperature for the InfoNCE loss is set to 0.6. Our model was pre-trained on SCT dataset.

Baselines. We consider several baselines for the pre-training task to evaluate whether the pair-matching task serves as a suitable proxy for the classification problem. Since the optimization problem is an unsupervised learning task, we compare it with both zero-shot (ANIL [32] and pre-trained BioGPT [26]) and few-shot (MAML [11]) learning approaches. To train these meta-learning models, we further split the TOP benchmark into different meta-tasks based on chronological order. For each meta-task, there are 100 clinical trials, from which we randomly select 10 for the support set and the remaining 90 for the query set. We train ANIL (zero-shot) and MAML (few-shot) models as baselines using this split. Additionally, we consider the pre-trained BioGPT (zero-shot) as another baseline. Description and implementation details can be found in Appendix C.1.

Evaluation. All results from the pre-training stage are evaluated on the query set of the TOP benchmark. MAML is the only method that uses the support set during testing.

PEFT Stage. Our model. We add a prediction head, consisting of a 3-layer feed-forward neural network with ReLU activation and residual connections. LoRA layers with a rank size of 8 are added to all attention layers in the DM branch. The best model parameters from pre-training stage are used as the initial weights, and we continue training only the prediction head and LoRA layers.

Optimization. We use the Adam optimizer with default values for β_1 and β_2 . The batch size is set to 128, with a fixed learning rate of 10^{-2} for the prediction head, and 5×10^{-2} for the LoRA layers during phase I and phase II, 10^{-3} for the phase III training.

Baselines. We compare CLaDMoP with several baselines often evaluated on the TOP benchmark, including Logistic Regression (LR), Random Forest (RF), k-Nearest Neighbor + Random Forest (kNN+RF), XGBoost, Adaptive Boosting (AdaBoost), a 3-layer Feed-Forward Neural Network (FFNN), HINT [12] and MEXA-CTP [45]. Detailed information can be found in the Appendix C.2.

Evaluation. We use bootstrapping to evaluate the model performance 10 times on a random selection of 80% of the test data to report the mean and standard deviation of the evaluation metrics.

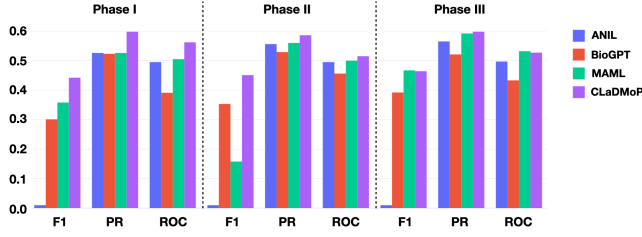


Figure 4: Few-shot learning results for clinical trial outcome prediction for phase I, II and III trials.

Table 3: Evaluation results comparing MEXA-CTP and CLaDMoP on new diseases. Best results are highlighted in bold.

	Method	F1	PR-AUC	ROC-AUC	ACC	Gain
Phase I	MECA-CTP	.428	.522	.517	47.55	
	CLaDMoP	.448	.535	.520	54.34	+9
Phase II	MECA-CTP	.471	.569	.536	55.00	
	CLaDMoP	.499	.594	.562	59.41	+15
Phase III	MECA-CTP	.461	.554	.528	55.55	
	CLaDMoP	.447	.576	.529	54.34	-3

4.2 Experiment Results

Pre-training Results. Figure 4 shows the comparison results for each phase. The performance gaps over the best-performing baseline (MAML) are larger in the first two phases: 23.5% and 184.8% for F1; 13.7% and 4.6% for PR-AUC; and 11.3% and 3.0% for ROC-AUC. The performance gaps over MAML are smaller in phase III, as the dataset grows larger, allowing MAML to learn more effectively from the support task. From the training perspective, our model is more stable than MAML and ANIL across all phases training. As shown later, our pre-trained model outperforms even some supervised models, demonstrating the effectiveness of our approach.

Fine-tuning Results. Table 2 shows the comparison results for phase I, phase II, and phase III including standard deviation values obtained via bootstrapping. For all phases, CLaDMoP consistently achieves the best performance in terms of PR-AUC and ROC-AUC, immediately followed by MEXA-CTP. For comparison purposes, we compute simple (unweighted) averages of their performance differences across phases. On average, CLaDMoP achieves 10.5% and 3.6% higher PR-AUC and ROC-AUC, while maintaining a comparable F1 score to that of MEXA-CTP.

New Diseases. We select disease combinations $\mathcal{D}^{(j)}$ that appear ONLY in test sets but not in ANY training set, referring to them as “New Diseases”. Detailed statistics are provided in Appendix B.2. We compare our results with the previous SOTA, MEXA-CTP on the subset of new diseases. Table 3 shows, in addition to the previously used evaluation metrics, the gain in the number of correct predictions. CLaDMoP consistently outperforms MEXA-CTP in F1, PR-AUC, and ROC-AUC in both Phase I and Phase II, especially achieving 13.63% higher accuracy in Phase I and 8.02% in Phase II, while matching MEXA-CTP’s performance in Phase III.

4.3 Ablation Studies

We conduct ablation studies for assessing (i) the importance of using multiple grouping blocks, (ii) the gains from the fine-tuning stage via LoRA, (iii) the necessity of incorporating a pre-training stage, and (iv) the proposed strategy for dataset usage in pre-training and fine-tuning stage. For these studies, we focus on the results for phase III, using the best hyperparameters obtained in Section 4.1, unless stated otherwise.

Table 4: Ablation studies for the Grouping Block configuration. S indicates the number of the self-attention layer(s) in a grouping layer, and G indicates the number of the grouping layer(s) in a grouping block. CLaDMoP uses $G = 3, S = 2$.

Method	F1	PR-AUC	ROC-AUC
$G=1, S=2$.797±.011	.808±.015	.611±.015
$G=2, S=2$.836±.009	.803±.014	.642±.011
$G=3, S=0$.612±.011	.669±.015	.615±.023
$G=3, S=1$.773±.018	.813±.015	.618±.016
$G=3, S=3$.692±.015	.857±.006	.698±.015
CLaDMoP	.861 ±.014	.860±.014	.702±.018

Grouping Block Setting. We consider two main configurations for the setting of Grouping Block: (i) the number of S self-attention layer(s) in a grouping layer, where $S \in \{0, 1, 2, 3\}$, and (ii) the number of G grouping layer(s) in a grouping block, where $G \in \{1, 2, 3\}$. Our design, with $G = 3, S = 2$, yields the best performance compared to other configurations. In all cases, the final number of the centroids is fixed to 25. For example, $G = 3, S = 2$ indicates that, in each grouping layer, the cross-attention layer is followed by two self-attention layers, and for each grouping block, CLaDMoP is initialized with 100 centroids, then halved to 50 centroids, and subsequently to 25 centroids.

Table 5: Ablation studies for importance of introducing LoRA in fine-tuning stage. CLaDMoP uses head + X_{LoRA} + S_{LoRA} .

Method	F1	PR-AUC	ROC-AUC
head-only	.806 ±.012	.857±.014	.675±.011
head+ X_{LoRA}	.822 ±.012	.856±.014	.681±.024
head+ S_{LoRA}	.851 ±.009	.860±.012	.700±.016
CLaDMoP	.861 ±.014	.860±.011	.702±.018

Fine-tuning with LoRA. To further improve performance, we incorporate LoRA layers into the DM branch. We consider three alternative configurations for PEFT: (i) training only the parameters of the prediction head (head-only); (ii) training both the prediction head and LoRA layers in the cross-attention layer (head + X_{LoRA}); and (iii) training both the prediction head and LoRA layers in the self-attention layers for embedding enrichment (head + S_{LoRA}). As shown in Table 5, training the prediction head and both LoRA layers from the grouping layer (i.e., as done in CLaDMoP) results in a significant performance boost, with a 1.2% improvement in F1 score and a 2.9% in ROC-AUC over the second best configuration.

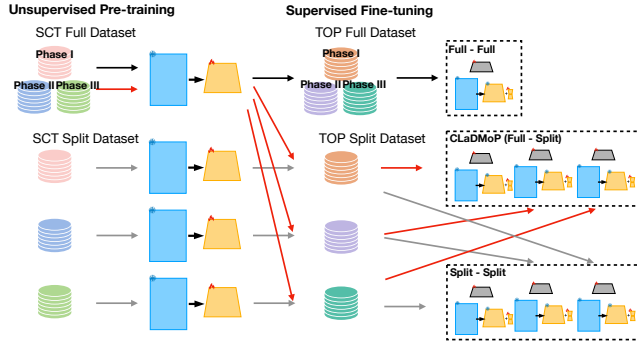


Figure 5: We show three different training strategies for model development, showing the dataflow during both pre-training and fine-tuning stages. The arrows represent the path of the data usage for each strategy: (i) Split-Split Training Strategy, where separate models are trained on different phases in SCT and then fine-tuned on the corresponding phases in TOP; (ii) Black Arrows: Full-Full training strategy, where the entire SCT is used for pre-training and entire TOP is used for fine-tuning; (iii) Red Arrows: Full-Split Training Strategy, where the entire SCT dataset is used for pre-training, while fine-tuning is performed on phase-specific TOP dataset.

Training strategy. We evaluate two alternative training strategies and compare them with our model: (i) using the pre-trained model directly without further fine-tuning and evaluating pair-matching results, and (ii) fine-tuning the model without a pre-training stage. As shown in Table 6, our training strategy (pre-training + fine-tuning) consistently outperforms the other two approaches.

Table 6: Ablation studies for the necessity of combining both pre-training and fine-tuning stages.

Method	F1	PR-AUC	ROC-AUC
w/o fine-tuning	.357 ± .008	.466 ± .009	.514 ± .010
w/o pre-training	.800 ± .013	.766 ± .12	.680 ± .010
CLaDMoP	.861 ± .014	.860 ± .011	.702 ± .018

Dataset Usage in Pre-Training and Fine-Tuning. We analyze the impact of alternative strategies for using the SCT data during pre-training and the TOP data dataset during fine-tuning. In the pre-training stage, we explore two approaches: (i) split the SCT data by trial phase to train phase-specific models, or (ii) use the full data (i.e., including all samples across phases I, II and III) to train a single, general model. In the first case, it is natural to fine-tune each model variant by also splitting the TOP data accordingly—we call this strategy **Split-Split**. In the second case, we can take the phase-agnostic model and fine-tune it on the TOP full data—we call this strategy **Full-Full**, instead of splitting the TOP data as done in CLaDMoP. A sketch of the three strategies can be found in Fig. 5. *Pre-training.* To highlight the advantages of using a large dataset for the pre-training stage, we compare models trained on SCT

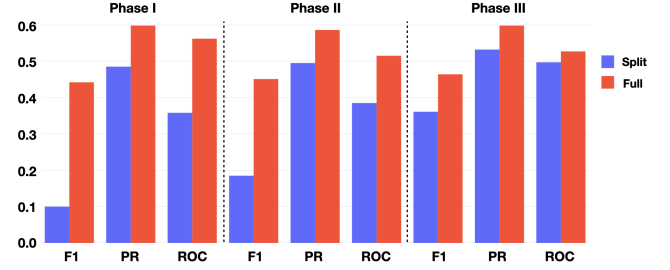


Figure 6: Pre-trained models performance using SCT *split* by clinical phase vs. the *full* SCT dataset (which benefits from having more data).

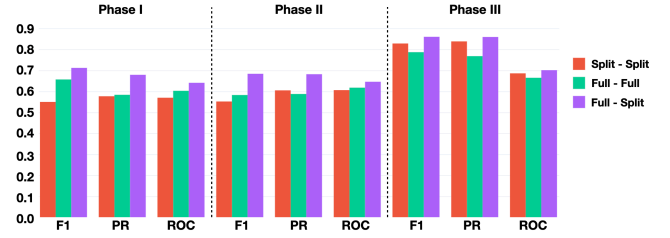


Figure 7: (PEFT) fine-tuned models performance for three data usage strategies: 1st term in the key indicates if models were pre-trained on SCT split or SCT full; 2nd term indicates if they were fine-tuned on TOP split or TOP full. We found that Full - Split (CLaDMoP’s strategy) performed best.

split dataset with the model trained on SCT full dataset, as shown in Fig. 6. CLaDMoP’s strategy, i.e., training on SCT full, achieves improvements of 342%, 144%, 28.5% in F1, 23.3%, 18.4%, 12.4% in PR-AUC and 57.0%, 33.8%, 6.0% in ROC-AUC for phases I, II, and III, respectively. The benefit of SCT full dataset is particularly significant when there are limited samples available in each phase. *PEFT.* We compare fine-tuned models using alternative data usage strategies—namely, Full-Full and Split-Split—with CLaDMoP. Our training strategy (i.e., pre-training with the SCT full dataset and fine-tuning with the TOP split dataset) consistently achieves the best performance across phases I, II, and III, as shown in Fig. 7.

4.4 Complexity Analysis

As a transformer-based model, CLaDMoP’s time complexity for training is $O(dn^2)$, where d is the hidden size of the attention model, n is the sequence length. Since the LLM branch uses a decoder-only model, in most cases the number of tokens from this branch largely exceeds those fused with the DM branch. Therefore, CLaDMoP fuses information from the LLM branch into the DM branch, causing the sequence length to grow linearly with the number of fusion steps. As a result, the attention computation in the DM branch scales quadratically. However, our grouping blocks help maintain the token sequence length at a predefined value of 25, preventing quadratic growth in computation and significantly reducing the computational cost [43].

5 RELATED WORK

Clinical Trial Outcome Prediction. Many studies have focused on predicting individual patient outcomes within clinical trials through patient retrieval and enrollment information, rather than predicting overall trial success. For instance, Doctor2Vec [1] learns representations for medical providers and trials from electronic health records (EHR) and trial descriptions to address issues like recruitment in less populated countries. DeepEnroll [44] encodes enrollment criteria and patient records into a shared latent space for matching, while COMPOSE [13] uses medical ontology-based patient records and eligibility criteria embeddings for dynamic patient-trial matching. More recently, a few methods were proposed to directly predict clinical trial outcomes based on drug molecules, target diseases, and eligibility criteria. Hong et al. [16] focused on forecasting clinical drug toxicity using features related to drug and target properties, employing an ensemble classifier of weighted least squares support vector regression. RS-RNN [29] predicted phase III outcomes based on phase II results by considering time-invariant and time-variant variables. EBM-Net [21] inferred clinical trial outcomes by unstructured sentences from medical literature that implicitly contain PICO (Population, Intervention, Comparison and outcome). More recently, HINT [12] incorporated drug molecule features, target diseases, and eligibility criteria to design a neural network which consists of several modules connected as a graph encoding human priors. MEXA-CTP [45] predicts clinical trial outcome using same input as HINT but with minimal human efforts by learning to select a relevant subset of tokens via mode experts. Our method, CLaDMoP, incorporates a pre-training stage [19] using unlabeled data [20, 42], followed by a fine-tuning stage to further enhance performance. This two-stage training approach significantly improves the robustness of the embeddings and the model’s predictive power. Meanwhile CLaDMoP utilize the grouping layers to reduce computational costs [18].

Large Language Models for Clinical Trials. There is significant interest in leveraging Large Language Models (LLMs) for various prediction tasks in the context for clinical trials [46]. They have been applied with mixed success for structuring eligibility criteria through logic operators and matching patients to clinical trials [39, 41], and are currently under consideration for assisting in clinical trial planning, coding-free text narratives and other side tasks. There is significant interest in leveraging Large Language Models (LLMs) for various prediction tasks in the context for clinical trials [46]. They have been applied with mixed success for structuring eligibility criteria through logic operators and matching patients to clinical trials [39, 41], and are currently under consideration for assisting in clinical trial planning, coding free text narratives and other side tasks. For clinical trial outcome prediction, however, it is not possible to directly use extant, subscription-based APIs (e.g., ChatGPT), due to their inability to handle some data modalities (e.g., drug molecules and ICD codes). Nevertheless, recently released open-source LLMs (e.g., Llama [37]) can be, in theory, trained to deal with such inputs [25, 35, 40]. However, a number of formidable challenges must be overcome first: (i) the immense amount of data required to train large models from scratch, since models pre-trained on human language cannot be directly fine-tuned for this purpose; (ii) the risk of hallucinations, which require finding new

ways of grounding the output produced by LLMs; (iii) the societal biases learned during training, which can lead to unfair outcomes, especially in critical areas like healthcare [34]. As a result, there is still much debate around the regulation of the use of such models in the medical domain [30].

6 CONCLUSION

Our approach demonstrates the potential of self-supervised learning to improve clinical trial outcome prediction with limited labeled data. With a two-branch architecture, we employ contrastive learning between LLM branch and DM branch using an adapted InfoNCE loss, allowing the model to learn robust task-agnostic representations. To support pre-training, we collect a new dataset, titled Successful Clinical Trials (SCT). Additionally, we leverage intermediate embeddings from the LLM branch through efficient information-fusion blocks (grouping blocks). Each grouping block consists of several grouping layers, which progressively reduce the token sequence length, enabling enhanced performance while minimizing computational costs. Our pre-trained model demonstrates significant improvements over established zero-shot and few-shot baselines based on evaluation across three clinical trial phases. We further improve the performance on the Trial Outcome Prediction (TOP) benchmark by training LoRA layers on the DM branch and a prediction head. CLaDMoP achieves up to 10.5% and 3.6% improvements in PR-AUC and ROC-AUC, respectively, while maintaining a comparable F1 score to MEXA-CTP. We also analyze the accuracy and the absolute gain in correct predictions for new diseases compared to the previous state-of-the-art MEXA-CTP, showcasing that CLaDMoP can learn generalizable embeddings via task-agnostic loss and easily adapt to new drug molecules. This method sets a promising direction for further advancements in clinical trial prediction using deep learning.

REFERENCES

- [1] Siddharth Biswal, Cao Xiao, Lucas M Glass, Elizabeth Milkovits, and Jimeng Sun. 2020. Doctor2vec: Dynamic doctor representation learning for clinical trial recruitment. In *AAAI*.
- [2] Wendy M Bjornson-Benson, Thomas B Stibolt, Kenneth A Manske, Kathleen J Zavela, Diana J Youtsey, and A Sonia Buist. 1993. Monitoring recruitment effectiveness and cost in a clinical trial. *Controlled clinical trials* 14, 2 (1993), 52–67.
- [3] Daniel Bobo, Kye J Robinson, Jiaul Islam, Kristofer J Thurecht, and Simon R Corrie. 2016. Nanoparticle-based medicines: a review of FDA-approved materials and clinical trials to date. *Pharmaceutical research* 33 (2016), 2373–2387.
- [4] Changyou Chen, Jianyi Zhang, Yi Xu, Liqun Chen, Jiali Duan, Yiran Chen, Son Tran, Belinda Zeng, and Trishul Chilimbi. 2022. Why do we need large batch-sizes in contrastive learning? a gradient-bias perspective. *Advances in Neural Information Processing Systems* 35 (2022), 33860–33875.
- [5] Shein-Chung Chow and Annpay Pong. 1998. An overview of the regulatory approval process in drug development. *Drug information journal* 32, 1_suppl (1998), 1175S–1185S.
- [6] Joseph A DiMasi, Ronald W Hansen, and Henry G Grabowski. 2003. The price of innovation: new estimates of drug development costs. *Journal of health economics* 22, 2 (2003), 151–185.
- [7] Nicholas S Downing, Jenerius A Aminawung, Nilay D Shah, Harlan M Krumholz, and Joseph S Ross. 2014. Clinical trial evidence supporting FDA approval of novel therapeutic agents, 2005–2012. *Jama* 311, 4 (2014), 368–377.
- [8] Sarah A Dugger, Adam Platt, and David B Goldstein. 2018. Drug development in the era of precision medicine. *Nature reviews Drug discovery* 17, 3 (2018), 183–196.
- [9] Harold Edgar and David J Rothman. 2018. New rules for new drugs: the challenge of AIDS to the regulatory process. In *AIDS: Society, Ethics and Law*. Routledge, 447–478.
- [10] Lijie Fan, Dilip Krishnan, Phillip Isola, Dina Katabi, and Yonglong Tian. 2023. Improving clip training with language rewrites. *Advances in Neural Information Processing Systems* 36 (2023), 35544–35575.
- [11] Chelsea Finn, Pieter Abbeel, and Sergey Levine. 2017. Model-agnostic meta-learning for fast adaptation of deep networks. In *International conference on machine learning*. PMLR, 1126–1135.
- [12] Tianfan Fu, Kexin Huang, Cao Xiao, Lucas M Glass, and Jimeng Sun. 2022. Hint: Hierarchical interaction network for clinical-trial-outcome predictions. *Patterns* 3, 4 (2022).
- [13] Junyi Gao, Cao Xiao, Lucas M Glass, and Jimeng Sun. 2020. COMPOSE: Cross-modal pseudo-siamese network for patient trial matching. In *KDD*. 803–812.
- [14] Luyu Gao, Yunyi Zhang, Jiawei Han, and Jamie Callan. 2021. Scaling deep contrastive learning batch size under memory limited setup. *arXiv preprint arXiv:2101.06983* (2021).
- [15] Zeyu Han, Chao Gao, Jinyang Liu, Jeff Zhang, and Sai Qian Zhang. 2024. Parameter-efficient fine-tuning for large models: A comprehensive survey. *arXiv preprint arXiv:2403.14608* (2024).
- [16] Zhen-Yu Hong, Jooyong Shim, Woo Chan Son, and Changha Hwang. 2020. Predicting successes and failures of clinical trials with an ensemble LS-SVR. *medRxiv* (2020).
- [17] Edward J Hu, Yelong Shen, Phillip Wallis, Zeyuan Allen-Zhu, Yuanzhi Li, Shean Wang, Lu Wang, and Weizhu Chen. 2021. Lora: Low-rank adaptation of large language models. *arXiv preprint arXiv:2106.09685* (2021).
- [18] Mingzhi Hu, Xin Zhang, Yanhua Li, Yiqun Xie, Xiaowei Jia, Xun Zhou, and Jun Luo. 2024. Only Attending What Matter within Trajectories–Memory-Efficient Trajectory Attention. In *Proceedings of the 2024 SIAM International Conference on Data Mining (SDM)*. SIAM, 481–489.
- [19] Mingzhi Hu, Zhuoyun Zhong, Xin Zhang, Yanhua Li, Yiqun Xie, Xiaowei Jia, Xun Zhou, and Jun Luo. 2023. Self-supervised pre-training for robust and generic spatial-temporal representations. In *2023 IEEE International Conference on Data Mining (ICDM)*. IEEE, 150–159.
- [20] Ruofan Hu, Dongyu Zhang, Dandan Tao, Huayi Zhang, Hao Feng, and Elke Rundensteiner. 2023. Uce-fid: Using large unlabeled, medium crowdsourced-labeled, and small expert-labeled tweets for foodborne illness detection. In *2023 IEEE International Conference on Big Data (BigData)*. IEEE, 5250–5259.
- [21] Qiao Jin, Chuanqi Tan, Mosha Chen, Xiaozhong Liu, and Songfang Huang. 2020. Predicting Clinical Trial Results by Implicit Evidence Integration. *arXiv preprint arXiv:2010.05639* (2020).
- [22] Sravya Kakumanu, Braden J Manns, Sophia Tran, Terry Saunders-Smith, Brenda R Hemmelgarn, Marcello Tonelli, Ross Tsuyuki, Noah Ivers, Danielle Southern, Jeff Bakal, et al. 2019. Cost analysis and efficacy of recruitment strategies used in a large pragmatic community-based clinical trial targeting low-income seniors: a comparative descriptive analysis. *Trials* 20 (2019), 1–12.
- [23] Richard L Kravitz, Naihua Duan, and Joel Braslow. 2004. Evidence-based medicine, heterogeneity of treatment effects, and the trouble with averages. *The Milbank Quarterly* 82, 4 (2004), 661–687.
- [24] Robert J Levine. 1988. *Ethics and regulation of clinical research*. Yale University Press.
- [25] Yuhang Liu, Yingxue Zhang, Xin Zhang, Ling Tian, Xu Zheng, Yanhua Li, and Jun Luo. 2025. UrbanMind: Urban Dynamics Prediction with Multifaceted Spatial-Temporal Large Language Models. *arXiv preprint arXiv:2505.11654* (2025).
- [26] Renqian Luo, Liai Sun, Yingce Xia, Tao Qin, Sheng Zhang, Hoifung Poon, and Tie-Yan Liu. 2022. BioGPT: generative pre-trained transformer for biomedical text generation and mining. *Briefings in bioinformatics* 23, 6 (2022), bbac409.
- [27] Thamsanqa Mlotshwa, Heinrich van Deventer, and Anna Sergeevna Bosman. 2022. Cauchy Loss Function: Robustness Under Gaussian and Cauchy Noise. In *SACAIR*.
- [28] Aaron van den Oord, Yazhe Li, and Oriol Vinyals. 2018. Representation learning with contrastive predictive coding. *arXiv preprint arXiv:1807.03748* (2018).
- [29] Youran Qi and Qi Tang. 2019. Predicting phase 3 clinical trial results by modeling phase 2 clinical trial subject level data using deep learning. In *MLHC*.
- [30] Jianing Qiu, Wu Yuan, and Kyle Lam. 2024. The application of multimodal large language models in medicine. *The Lancet Regional Health–Western Pacific* (2024).
- [31] Alec Radford, Jong Wook Kim, Chris Hallacy, Aditya Ramesh, Gabriel Goh, Sandhini Agarwal, Girish Sastry, Amanda Askell, Pamela Mishkin, Jack Clark, et al. 2021. Learning transferable visual models from natural language supervision. In *International conference on machine learning*. PMLR, 8748–8763.
- [32] Aniruddh Raghu, Maithra Raghu, Samy Bengio, and Oriol Vinyals. 2019. Rapid learning or feature reuse? towards understanding the effectiveness of maml. *arXiv preprint arXiv:1909.09157* (2019).
- [33] Bharath Ramsundar. 2018. *Molecular machine learning with DeepChem*. Ph. D. Dissertation. Stanford University.
- [34] Chiman Salavati, Shannon Song, Willmar Sosa Diaz, Scott A Hale, Roberto E Montenegro, Fabricio Murai, and Shiri Dori-Hacohen. 2024. Reducing biases towards minoritized populations in medical curricular content via artificial intelligence for fairer health outcomes. In *Proceedings of the AAAI/ACM Conference on AI, Ethics, and Society*, Vol. 7. 1269–1280.
- [35] Neil Savage. 2023. Drug discovery companies are customizing ChatGPT: here's how. *Nature Biotechnology* (2023).
- [36] Quan Sun, Yuxin Fang, Ledell Wu, Xinlong Wang, and Yue Cao. 2023. Eva-clip: Improved training techniques for clip at scale. *arXiv preprint arXiv:2303.15389* (2023).
- [37] Rohan Taori, Ishan Gulrajani, Tianyi Zhang, Yann Dubois, Xuechen Li, Carlos Guestrin, Percy Liang, and Tatsunori B Hashimoto. 2023. Stanford alpaca: An instruction-following llama model.
- [38] Craig A Umscheid, David J Margolis, and Craig E Grossman. 2011. Key concepts of clinical trials: a narrative review. *Postgraduate medicine* (2011).
- [39] Cliff Wong, Sheng Zhang, Yu Gu, Christine Moun, Jacob Abel, Naoto Usuyama, Roshanthi Weerasinghe, Brian Piening, Tristan Naumann, Carlo Bifulco, and Hoifung Poon. 2023. Scaling Clinical Trial Matching Using Large Language Models: A Case Study in Oncology. In *MLHC*.
- [40] Yang Wu, Huayi Zhang, Yizheng Jiao, Lin Ma, Xiaozhong Liu, Jinhong Yu, Dongyu Zhang, Dezhi Yu, and Wei Xu. 2024. ROSE: A Reward-Oriented Data Selection Framework for LLM Task-Specific Instruction Tuning. *arXiv preprint arXiv:2412.00631* (2024).
- [41] Jiayi Yuan, Ruixiang Tang, Xiaoqian Jiang, and Xia Hu. 2023. Large language models for healthcare data augmentation: An example on patient-trial matching. In *AMIA Annual Symposium Proceedings*.
- [42] Huayi Zhang, Lei Cao, Samuel Madden, and Elke Rundensteiner. 2021. Lancet: labeling complex data at scale. *Proceedings of the VLDB Endowment* 14, 11 (2021).
- [43] Xin Zhang, Yanhua Li, Ziming Zhang, Christopher Brinton, Zhenming Liu, Zhi-Li Zhang, Hui Lu, and Zhihong Tian. 2021. Stabilized Likelihood-based Imitation Learning via Denoising Continuous Normalizing Flow. (2021).
- [44] Xingyao Zhang, Cao Xiao, Lucas M Glass, and Jimeng Sun. 2020. DeepEnroll: patient-trial matching with deep embedding and entailment prediction. In *Web Conference*.
- [45] Yiqing Zhang, Xiaozhong Liu, and Fabricio Murai. 2025. MEXA-CTP: Mode Experts Cross-Attention for Clinical Trial Outcome Prediction. *arXiv preprint arXiv:2501.06823* (2025).
- [46] Ailin Zhao and Yijun Wu. 2023. Future implications of ChatGPT in pharmaceutical industry: drug discovery and development. *Frontiers in Pharmacology* (2023).

A ENCODING MODULE.

A.1 Drug Molecules Embedding.

We observe that although drug molecules may differ, they often share some SMILES segments. Therefore, we create molecule embeddings by intelligently combining their SMILES segment representations as obtained by DeepChem [33]. To improve efficiency, we build an embedding dictionary Dict_{emb} for each SMILES segment,

$$\text{Dict}_{\text{emb}} = \{e_{s_1}, e_{s_2}, \dots, e_{s_V}\}, \quad e_{s_k} = \text{DEEPCHEM}(s_k) \quad (8)$$

where $s_k; k \in [1..V]$ is a SMILES segment and e_{s_k} is the corresponding representation pre-computed by DEEPCHEM. Molecules embeddings are represented as a sequence of tokens from Dict_{emb} , denoted by $U_{\mathcal{M}(j)}$.

A.2 Target Diseases Embedding.

Each target disease in a trial is represented using the ICD-10 code tree, which expresses how different diseases and related within the disease classification system. We encode the structural information of each code using the ICDCODEX package:

$$U_{\mathcal{D}(j)} = \{e_{d_1^{(j)}}, e_{d_2^{(j)}}, \dots, e_{d_{D_j}^{(j)}}\}, \quad e_{d_i^{(j)}} = \text{ICDCODEX}(d_i^{(j)}), \quad (9)$$

$$i \in [1..D_j],$$

where $U_{\mathcal{D}(j)}$ represents a sequence of tokens for target disease embeddings.

A.3 Information Enrichment

We build a light weighted model for the Disease-Molecule branch. We enrich the representation from molecules embedding and disease embedding separately via self attention,

$$U_{\text{enriched}}^{\text{domain}} = \text{softmax} \left(\frac{U^{\text{domain}} W^Q (U^{\text{domain}} W^K)^T}{\sqrt{d_k}} \right) U^{\text{domain}} W^V, \quad (10)$$

where $\text{domain} \in \{\mathcal{M}, \mathcal{D}\}$.

B DATASET.

B.1 TOP dataset Statistics.

We provide the statistics for the TOP benchmark dataset in the table below.

Table 7: TOP benchmark dataset statistics.

Phase	Training	Test	Success Ratio
I	1,164	627	68%
II	4,451	1654	35%
III	4,313	1,146	30%

B.2 New Diseases Statistics.

New diseases are defined as combinations of diseases present in the test set but absent from all phases of the training set.

Table 8: New Diseases statistics.

Phase	New Disease	Test	Percentage
I	138	627	22%
II	340	1654	21%
III	198	1,146	17%

C BASELINES.

C.1 Pre-training baselines.

Model description

- **ANIL** focuses primarily on updating the last layer of the model (i.e., the task-specific part) while leaving the rest of the model’s parameters unchanged.
- **MAML** is to train a model on a distribution of tasks, such that it can adapt quickly to new, unseen tasks with minimal gradient updates.
- **BioGPT** is a question answering model pre-trained on large-scale biomedical corpora, including research papers, clinical trial reports, medical textbooks, and other domain-specific text sources.

ANIL & MAML. Implementation. We follow the approach outlined in the ANIL paper [32] and implement the code using PyTorch. All models consist of a 3-layer feed-forward neural network with ReLU activation functions.

Optimization. We applied class weight parameters to recalibrate the loss when the respective functions provided this hyperparameter. To gain best hyperparameters for each function in each phase, we employed cross-validation while training.

BioGPT. The conversation template with BioGPT model.

Algorithm 2 Conversation with LLMs

- 1: **System:** You are a clinical researcher.
- 2: **System:** I will give you CRITERIA, DISEASE, and DRUG for a clinical trial. Please give me an answer with “YES” or “NO” directly.
- 3: **User:** ELIGIBILITY: [eligibility criteria]
- 4: **User:** DISEASE: [name of target diseases]
- 5: **User:** DRUG: [name of drug compounds]
- 6: **Prompt:** Does the combination of the CRITERIA, DISEASE, and DRUG represent a good match in [phase] for predicting clinical outcomes?

C.2 Fine-tuning Baselines.

ML-based methods. Implementation. We utilized scikit-learn packages for all machine learning baselines, including Logistic Regression, Random Forest, k-Nearest Neighbor + Random Forest, XGBoost, Adaptive Boosting, a 3-layer Feed-Forward Neural Network. **Data Preprocessing.** We utilize the same encoding module outlined in MEXA-CTP [45]. For handling missing values, if the method involves k-nearest neighbors, we will generate k clusters using the non-missing values and predict the missing value based on the centroid of the corresponding cluster. For methods that do not incorporate clustering, we will substitute missing values with zeros.

Additionally, we will pad and chunk the array to ensure same size, using the normalized array as input for all the baseline models.

Optimization. We applied class weight parameters to recalibrate the loss when the respective functions provided this hyperparameter. To gain best hyperparameters for each function in each phase, we employed 5-fold cross-validation while training.

HINT. We strictly follow the HINT paper and their official GitHub⁹. **MEXA-CTP.** We strictly follow the MEXA-CTP paper and their official GitHub¹⁰.

C.3 Batch Size for Pre-training

The influence of the batch size affect the pre-training performance.

Batch Size in Pre-training. In previous studies [4, 14, 28], batch size has been shown to be a crucial hyperparameter in contrastive-based pre-training. ave demonstrated that batch size is a critical hyperparameter in contrastive-based pre-training. To achieve high-quality pre-training results, we experimented with different batch sizes to assess their impact on performance. As shown in Fig. 8, we choose a batch size of 128, which required 167 epochs to converge to the minimum validation loss.

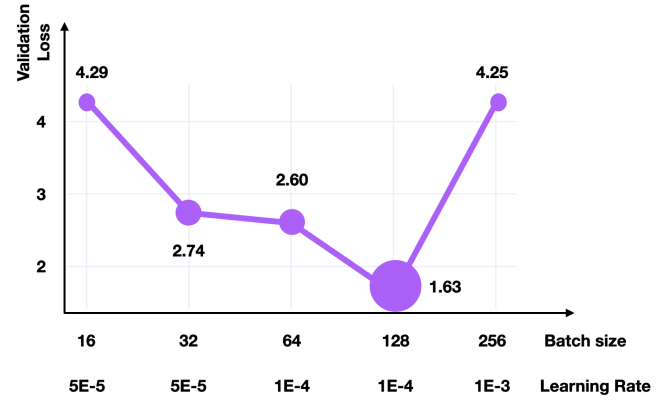


Figure 8: Batch size vs. validation loss. We show the corresponding learning rate for each batch size at the bottom of the figure. The size of the ball indicates the number of epochs required to reach the minimum validation loss.

Received 10 February 2025; revised 20 May 2025; accepted 16 May 2025

⁹<https://github.com/futianfan/clinical-trial-outcome-prediction>

¹⁰<https://github.com/murai-lab/>